![USGS logo](science for a changing world)

A Methodology for Modeling Barrier Island Storm-Impact Scenarios

By Rangley C. Mickey, Joseph W. Long, Nathaniel G. Plant, David M. Thompson, and P. Soupy Dalyander

U.S. Department of the Interior
U.S. Geological Survey

Contents

Figures

Table

Conversion Factors

International System of Units to U.S. customary units

Multiply	By	To obtain
Length		
meter (m)	3.281	foot (ft)
kilometer (km)	0.6214	mile (mi)
kilometer (km)	0.5400	mile, nautical (nmi)
meter (m)	1.094	yard (yd)

Datum

Vertical coordinate information is referenced to the North American Vertical Datum of 1988 (NAVD 88).

Horizontal coordinate information is referenced to the North American Datum of 1983 (NAD 83).

A Methodology for Modeling Barrier Island Storm-Impact Scenarios

By Rangley C. Mickey, Joseph W. Long, Nathaniel G. Plant, David M. Thompson, and P. Soupy Dalyander

Abstract

A methodology for developing a representative set of storm scenarios based on historical wave buoy and tide gauge data for a region at the Chandeleur Islands, Louisiana, was developed by the U.S. Geological Survey. The total water level was calculated for a 10-year period and analyzed against existing topographic data to identify when storm-induced wave action would affect island morphology. These events were categorized on the basis of the threshold of total water level and duration to create a set of storm scenarios that were simulated, using a high-fidelity, process-based, morphologic evolution model, on an idealized digital elevation model of the Chandeleur Islands. The simulated morphological changes resulting from these scenarios provide a range of impacts that can help coastal managers determine resiliency of proposed or existing coastal structures and identify vulnerable areas within those structures.

Introduction

Estimates of the response of beaches and barrier islands to storms are essential for the protection of infrastructure, recreation, and ecosystem services that these environments provide. Increases in wave heights and water levels associated with storm events can alter the coastal landscape, the severity of which depends on the degree to which the elevations of storm-driven water levels exceed threshold elevations of beaches and dunes (Long and others, 2014). With the impacts of climate change (e.g., sea level rise and potentially more intense or frequent tropical storms [Bender and others, 2010]), these thresholds may be exceeded more often than previously observed, presenting coastal managers and planners with difficult decisions related to the restoration of beaches and barrier islands (Williams, 2009). Thus, there is a need for methods of predicting coastal vulnerability and resiliency to a broad range of storm events that can assess current and proposed island configurations to aid in the decisionmaking process. A methodology to assess the impact of storms on barrier island systems was developed by the U.S. Geological Survey. The methodology is based on a representative set of realistic storm scenarios including (1) time series of waves and water levels, (2) merged, high-resolution topographic and bathymetric elevation data collected over different spatial and temporal scales, and (3) a high-fidelity, process-based, morphologic evolution model that resolves the interactions between storm waves and coastal features.

This storm-impact modeling framework is generic enough that it could be applied to any barrier island system where storm scenarios can be derived and elevation data are available. This approach could be used at locations with proposed or ongoing restoration projects to provide coastal managers a way of testing different engineering designs to see which design best meets project criteria (e.g., decreasing vulnerability to mild or extreme storms, maintaining suitable acreage above some threshold elevation for habitat, etc.). This framework could also be applied to existing, restored, or natural areas by updating the model with new topographic observations after new storm impacts occur and reanalyzing the expected storm response.

Study Area

The storm-impact modeling approach was developed and tested at the Chandeleur Islands, Louisiana. The Chandeleur Islands are a barrier island chain off the southeast coast of Louisiana (fig. 1) and span approximately 80 kilometers (km) from north to south. The islands were set aside in the early 1900s to form the Breton National Wildlife Refuge (BNWR) and serve as an essential refuge and breeding ground for migratory birds, such as the endangered piping plover (*Charadrius melodus*) and populations of brown pelicans (*Pelecanus occidentalis;* U.S. Fish & Wildlife Service, 2013).
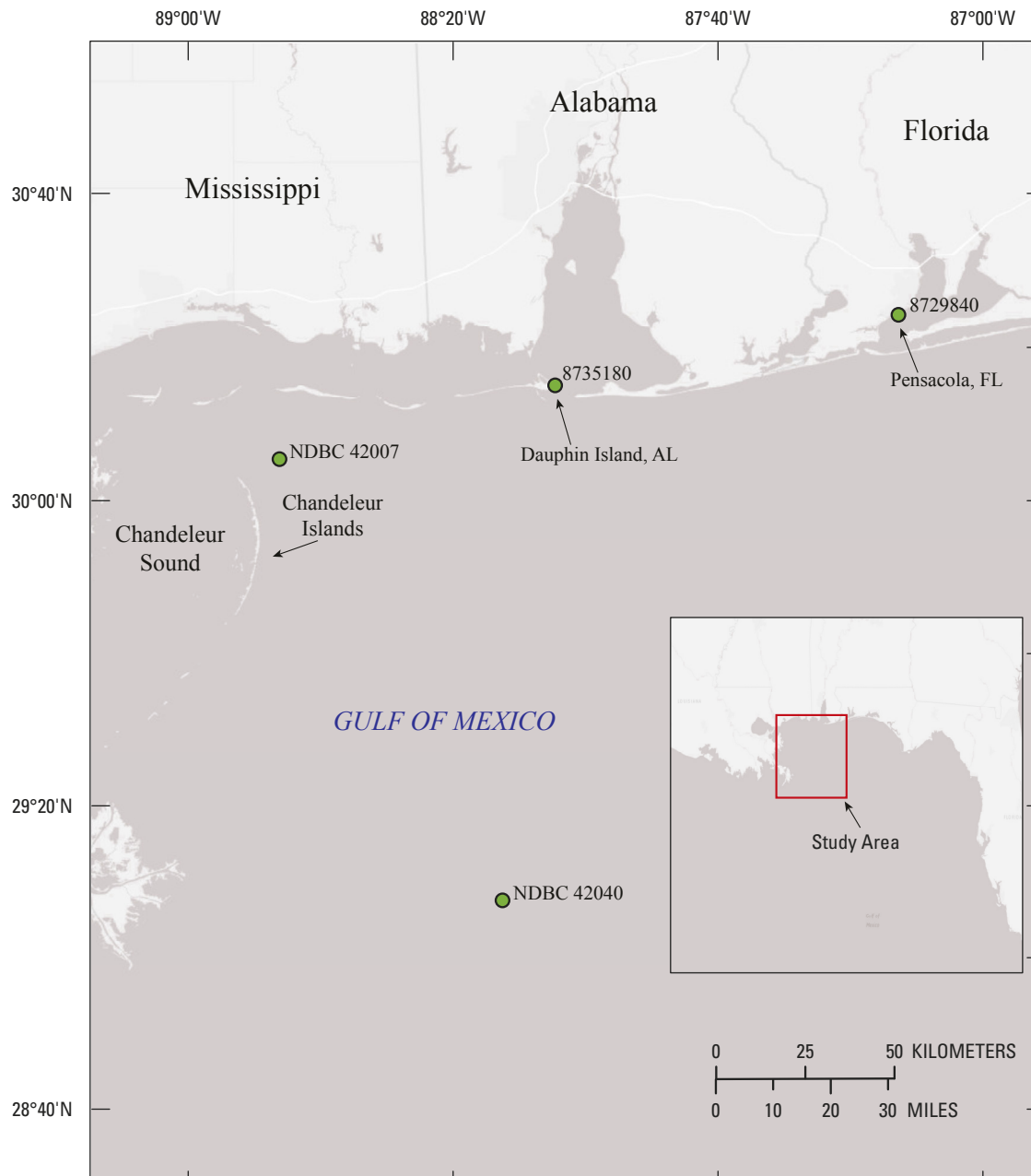
Figure 1. Location map of the Chandeleur Islands off the southeast coast of Louisiana. Green dots indicate wave and tide buoy locations.

In the past, this barrier island system has experienced an increasing amount of erosion due to the combination of major storm impacts (Penland and others, 1989) and limited natural recovery. The most significant changes to the island chain have occurred since the late 1990s due to the passage of multiple major storms including Hurricanes Georges (1998), Ivan (2004), and Katrina (2005) (Fearnley and others, 2009). The total island area was reduced by almost 50 percent from 1995 to 2005, with almost 90 percent removal of the sub-aerial sand volume (Fearnley and others, 2009).

The storm-impact approach is focused on the northern extent of the island chain (fig. 1) where a manufactured berm was constructed. In response to the April 2010 Deepwater Horizon oil spill, which occurred approximately 130 km southeast of the Chandeleur Islands, construction of an approximately 2-meter-(m) high sand berm along the gulf shoreline of the islands was proposed to prevent oil accumulation and impact (Louisiana Department of Natural Resources, 2010). Construction of the sand berm began in June 2010 and ended in March 2011. The entire berm feature was approximately 14 km long and spanned the northern extent of the island chain and the submerged island platform (fig. 2). The as-built berm can be divided into three sections based on proximity to the natural island: the northern section (~4 km long) is a standalone berm placed on top of the submerged relic island platform; the middle section (~3.5 km long) was built approximately 70–90 m seaward of the sub-aerial island; and the southern section (~6 km long) of the berm was built on top of the gulf side of the island (Plant and Guy, 2013a, 2013b, 2014).
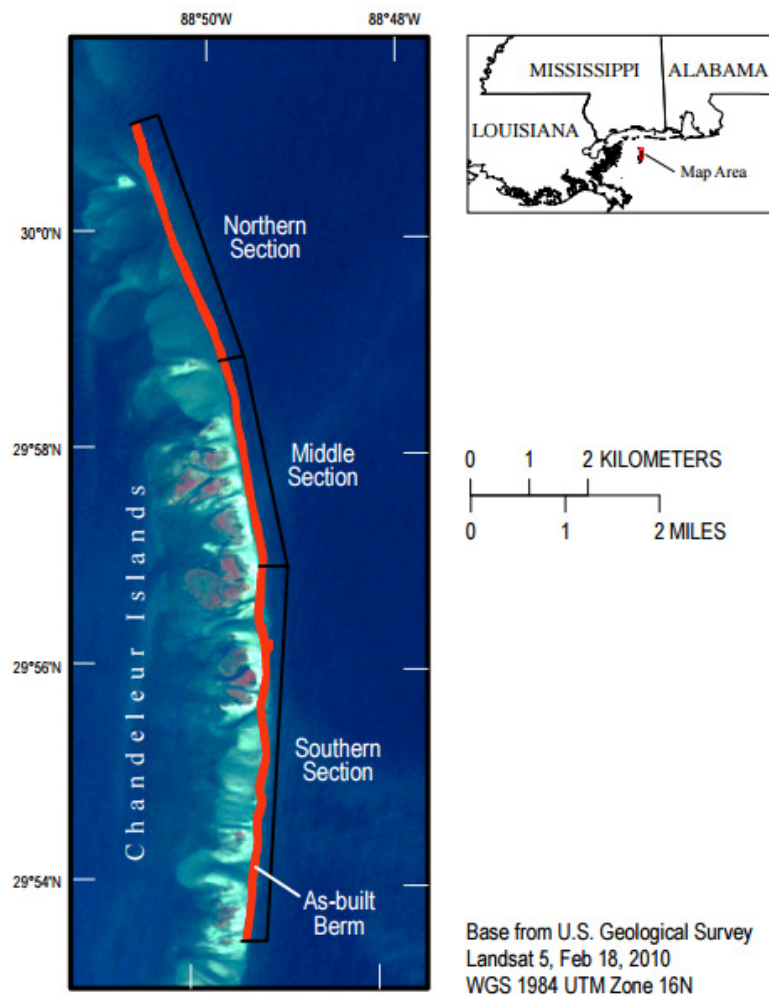
Figure 2. The Chandeleur Islands berm divided into northern, middle, and southern sections. The as-built berm footprint is shown in red. The background image is U.S. Geological Survey Landsat 5 taken February 18, 2010, prior to the start of berm construction (from Plant and Guy, 2013a).

Base from U.S. Geological Survey Landsat 5, Feb 18, 2010 WGS 1984 UTM Zone 16N

Methods

Described here are the details of the storm-impact approach: (1) how discrete storms were selected and binned to form a set of realistic storm scenarios, (2) development of the model hydrodynamic inputs and topographic/bathymetric grid, and (3) the model used to simulate morphological changes.

Representative Storm Scenarios

The impact of extreme storms on barrier islands is, for the most part, dictated by the magnitude and duration of elevated total water levels that occur during a storm. Total water levels (TWL) are defined as the combination of astronomical tides, storm surge, and wave-induced water levels including wave runup (Sallenger, 2000). The method used to develop the set of representative storms begins with calculating a time series of wave runup based on the basis of the parameterization developed by Stockdon and others (2006) that requires inputs of significant wave heights (H_s) and peak wave period (T_p) at an approximate water depth of 20 m and the foreshore beach slope. A 10-year (yr) (1996–2006) record of H_s and T_p was taken from the National Data Buoy Center's (NDBC) directional wave buoy 42007, previously located just northeast of the Chandeleur Islands (fig. 1) in 15 m water depth. The 10-yr recordings of H_s and T_p were interpolated to a uniform hourly time series; storm events or technical malfunctions periodically caused the buoy to go offline, which introduced data gaps. To create a continuous wave time series, a Bayesian model developed by Plant and others (2014) used offshore buoy data from NDBC buoy 42040 (237 m water depth) to predict H_s and T_p at the 42007 buoy location to fill in any data gaps (approximately 16 percent of the time series). The time series of both wave parameters were then smoothed over a 3 hour (h) window to decrease the effects of noisy data in the binning process.

The beach slope used for the wave runup calculation was derived from a light detection and ranging (lidar) survey conducted on September 4, 2010 (Fredericks and Plant, 2016); figure 3 shows the extent of the manufactured berm at that time. This survey was chosen because it incorporates a sizable section of the completed berm that had not been significantly degraded by storm impacts since the initial construction. The mean foreshore slope for the extent of the manufactured berm (–0.0174 m/m; fig. 3) was used along with the time series of H_s and T_p to generate the time series of wave runup.

The wave runup values were combined with hourly still-water measurements, which include the contribution of both astronomical tides and storm surge, taken from the Dauphin Island tide gauge (8735180; fig. 1) for the same 10-yr period to generate the time series of TWL. At times when the Dauphin Island gauge was unavailable, the Pensacola tide gauge (8729840; fig. 1) was used instead. These two gauges have been shown in previous studies to be well correlated (Wahl and Plant, 2015). The composite time series, originally referenced to Mean Sea Level (MSL), was converted to the North American Vertical Datum of 1988 (NAVD 88) for compatibility with the model topography and bathymetry described in the next section. For consistency, the still-water time series was also smoothed over a 3-h window before combination with the wave runup.

Within the 10-yr time period, a storm was defined as a time when oceanographic conditions were expected to cause morphological change to the berm feature. Hence, the TWL was compared to the average elevation of the base of the constructed sand berm (1.01 m), also extracted from the September 2010 lidar survey. This methodology identified time periods when water levels impacted the berm through processes like dune erosion, overwash, and inundation (Sallenger, 2000), all of which can be simulated in the numerical model described below. All time periods when the TWL reached or exceeded the base of the berm for a duration (D_s) of at least 6 continuous hours were identified as storms and used for defining the set of representative storm scenarios. If multiple events were identified within a
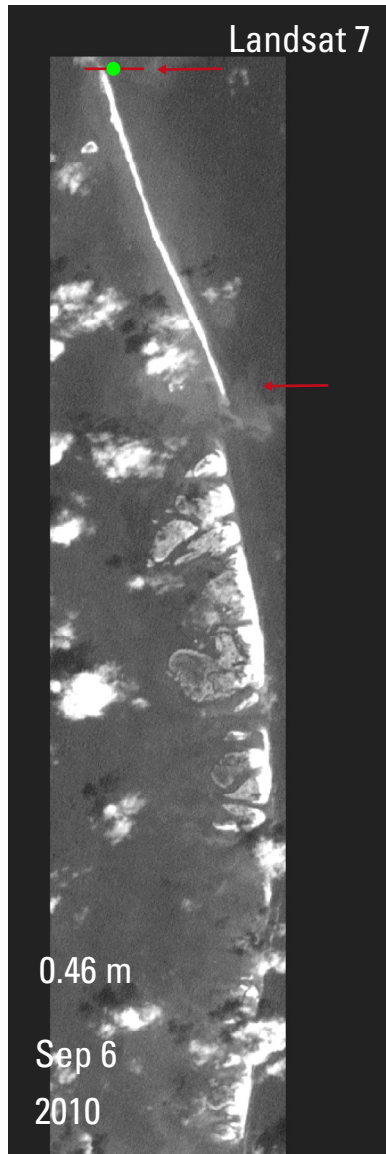
Figure 3. Landsat imagery of the berm on September 6, 2010, with a water level of 0.46 meter (NAVD 88). Green dot on red line indicates the location of the northern tip of the original constructed berm, and area between red arrows indicates length of berm used to calculate mean beach slope and berm toe.

24-h period, the events were combined along with the times when conditions were below the threshold. This process ensured that if events were identified at consecutive high tides but not during the intermediate low tide, they were not considered separate events (this area of the Gulf of Mexico has a diurnal tidal cycle). On the basis of this minimum threshold of TWL elevation and duration, a total of 28 individual events were identified from the 10-yr record.

Finally, all 28 storm events were assigned to scenarios by matching an event's maximum TWL and D_s to discrete TWL and D_s bins. Total water-level bins included five intervals: TWL > 1.01 m, TWL > 1.5 m, TWL > 2 m, TWL > 2.5 m, and TWL > 3 m. Storm D_s bins included four intervals: D_s > 6 h, D_s > 12 h, D_s > 24, and D_s > 36 h. The combination of TWL and D_s bins resulted in 20 storm scenario bins (fig. 4). The 28 storm events fell within 9 different bins (fig. 4; green boxes); 11 of the bins had no observable events (fig. 4; white boxes). The bin average and maximum values for H_s (meters), T_p (seconds), tide level (meters), D_s (hours), and TWL (meters) were calculated from the observed maximum of each event within that bin as well as the number of events observed in each bin (table 1).

5

Storm Scenario Bins
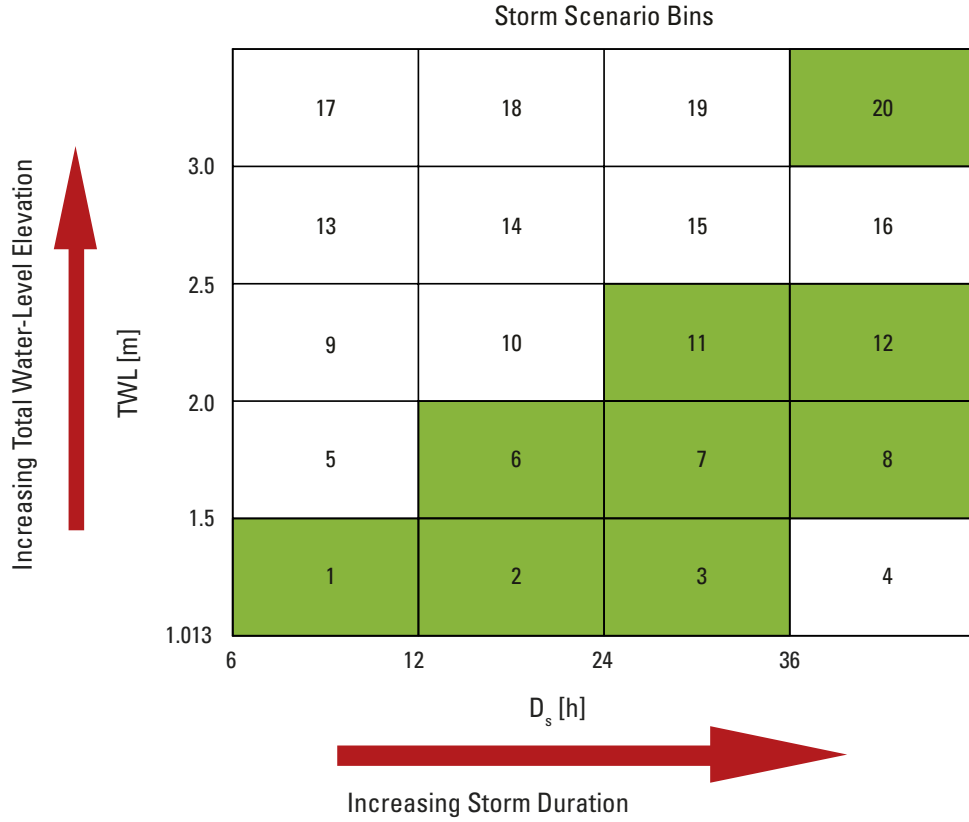
Figure 4. Representative storm scenario bins based on total water level, in meters (TWL [m]) and duration, in hours (D_s [h]). Green boxes denote bins that have observed events, and white boxes denote bins that do not have observed events. The numbers denote the storm scenario number.

Table 1. Storm bin characteristics.

[Bins where no events were observed are excluded. H_s, significant wave height; T_p, peak wave period; D_s, duration; TWL, total water level; m, meters; s, seconds; h, hours; --, only one event was observed, thus mean and max values are equal]

Bin	Events Observed	Mean H_s (m)	Max H_s (m)	Mean T_p (s)	Max T_p (s)	Mean Tide (m)	Max Tide (m)	Mean D_s (h)	Max D_s (h)	Mean TWL (m)	Max TWL (m)
1	13	2.30	3.15	9.2	11.1	0.46	0.58	8	11	1.13	1.21
2	3	3.15	3.96	10.7	11.0	0.48	0.55	14	15	1.33	1.39
3	3	3.04	3.29	9.5	11.1	0.56	0.60	28	30	1.17	1.20
6	2	2.85	3.14	10.9	11.7	0.68	0.72	14	16	1.57	1.61
7	1	3.49	--	12.3	--	0.67	--	30	--	1.60	--
8	1	3.30	--	9.4	--	0.71	--	37	--	1.50	--
11	1	3.63	--	13.5	--	0.80	--	33	--	2.06	--
12	3	4.74	4.87	13.3	14.3	1.23	1.48	61	67	2.38	2.49
20	1	7.78	--	16.7	--	1.62	--	45	--	3.71	--

Model Bathymetry and Topography

The long construction timeframe of 10 months coupled with natural evolution of the berm led to the inability to collect a complete survey of the as-built berm. To address this limitation, a model elevation grid was generated by merging available bathymetric survey data collected from 2006 to 2007 (Kindinger and others, 2013) and 2011 to 2012 (DeWitt and others, 2014a, b) with topographic lidar survey data collected from 2012 to 2013 (Guy and others, 2014a, b; Guy and Plant, 2014). In addition, satellite imagery, collected approximately every 2 weeks, from 2010 to 2011 was analyzed to outline the footprint of the fully constructed berm (fig. 2) (Plant and Guy, 2013a, b, 2014). The berm outline was used as a boundary to generate a Gaussian-shaped curve representing a 2-m-high berm, relative to NAVD 88, which was included in the process of merging all bathymetric and topographic surveys using the interpolation routines developed by Plant and others (2009). This merged topographic-bathymetric dataset provided a complete digital elevation model (DEM) of the manufactured berm based on the design criteria, the natural island, and the surrounding offshore and estuarine bathymetry (fig. 5). The berm feature developed through this process, therefore, may lack some alongshore variability that was present in the actual constructed berm feature.
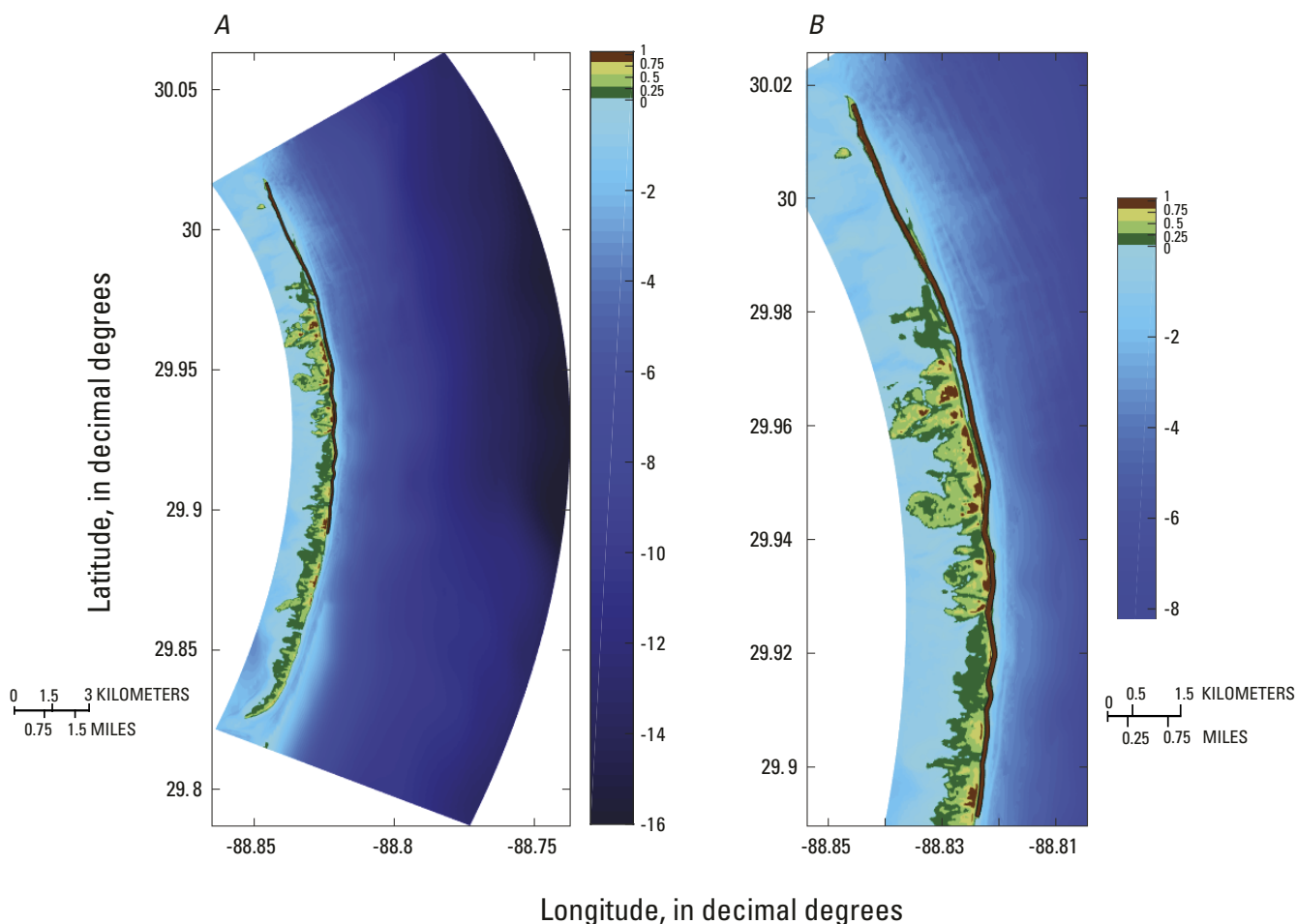

Figure 5.   (*A*) XBeach model domain and digital elevation model (DEM) of the Chandeleur Islands. (*B*) Zoomed version showing berm footprint outlined in black.

7

The cross-shore grid resolution increased logarithmically from offshore (~74 m) to onshore just seaward of the berm (2.5 m). Grid resolution is constant at 2.5 m across the island platform and back barrier, and the resolution decreases linearly through the sound to the western edge of the domain (~30 m). The representative conditions for each storm scenario were run using this merged DEM as the initial bathymetry and topography.

Numerical Model

The numerical model XBeach (version 4937) was used in this study to investigate how different storm scenarios impact the Chandeleur Islands' berm and adjacent areas. The XBeach model solves coupled two-dimensional, horizontal wave propagation equations to predict flow, sediment transport, and bottom changes for varying spectral wave and flow boundary conditions (Roelvink and others, 2009). The XBeach model setup requires the input of a merged topographic and bathymetric DEM, and inputs of wave spectra (based on H_s, T_p, and wave direction) and water level (tide and surge) time series at the seaward model boundary that span the duration of each storm bin. Because the duration of the event begins when the TWL reaches the minimum threshold, the time span used to extract the H_s, T_p, and water level from the 10-yr time series for each storm was extended 24 h prior to and after the event in order to capture the storm event ramp up and ramp down in the model run. The model input time series for each variable (H_s, T_p, and water level) was generated by averaging all the time series of that variable for the storms in each bin. For example, bin 1 contained 13 individual events; the time series of H_s, T_p, and water level of each of those 13 events were averaged to produce a mean time series for each variable (fig. 6).
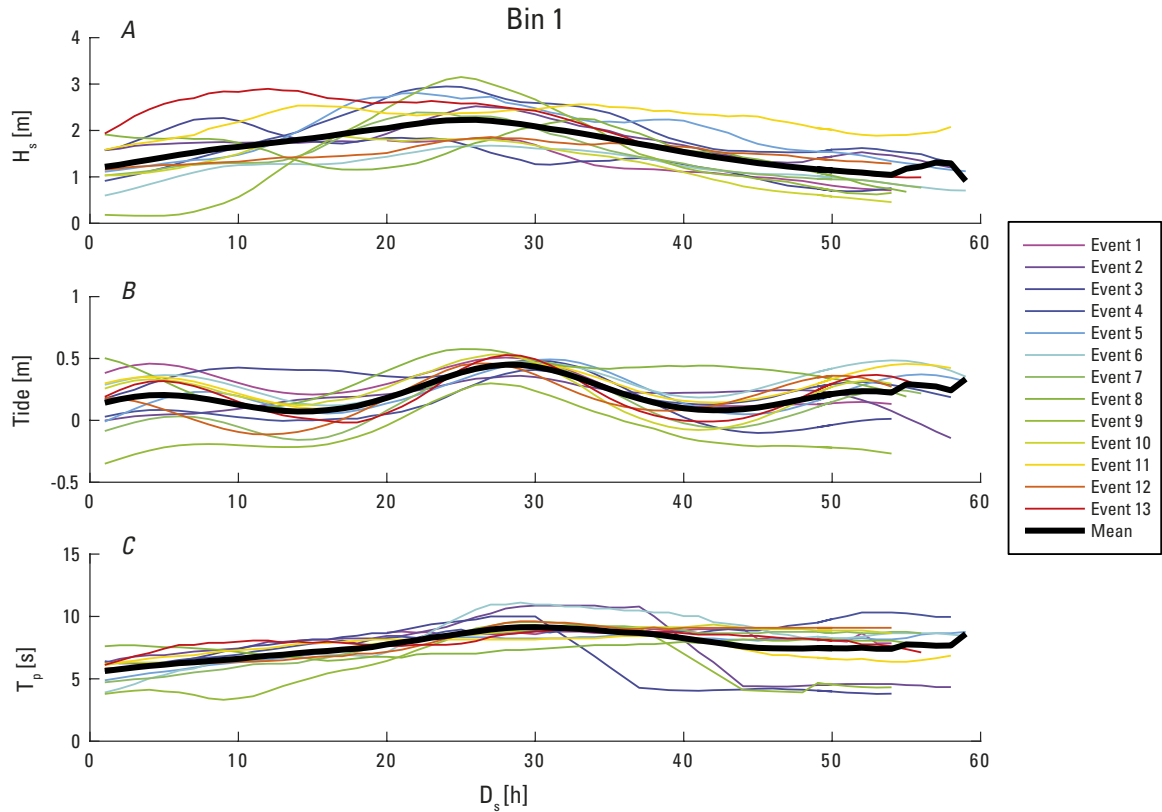

Figure 6. Time series, in hours (D_s [h]), of each of the 13 events in bin 1 for (*A*) significant wave height, in meters (H_s [m]), (*B*) Tide, in meters, and (*C*) peak wave period, in seconds (T_p [s]). The mean curve derived from averaging all 13 events is represented by the black line in each subplot.

8

For bins that had only one identified event, the observed time series extracted for each variable was used for model input. Incident wave direction was held at normally incident to the shoreline (90 degrees) for the duration of the model runs in order for the model results to reflect the maximum effect of wave/water-level impacts to the cross-shore island profiles. With the H_s and T_p time series for each scenario, along with constant wave direction, idealized hourly wave spectra were generated for the model assuming a parameterized Joint North Sea Wave Project (JONSWAP) spectrum (Hasselmann and others, 1973). Other inputs for the spectral wave files that did not vary among the scenarios were the model default peak enhancement factor (γ) of 3.3, the model directional spreading coefficient of 20, and the model default frequency range of 0–0.3 hertz. The time series of tides/surge was applied to the western (backside of island) and eastern (offshore) boundaries (fig. 6B). Examples of the XBeach input files are provided in appendix 1.
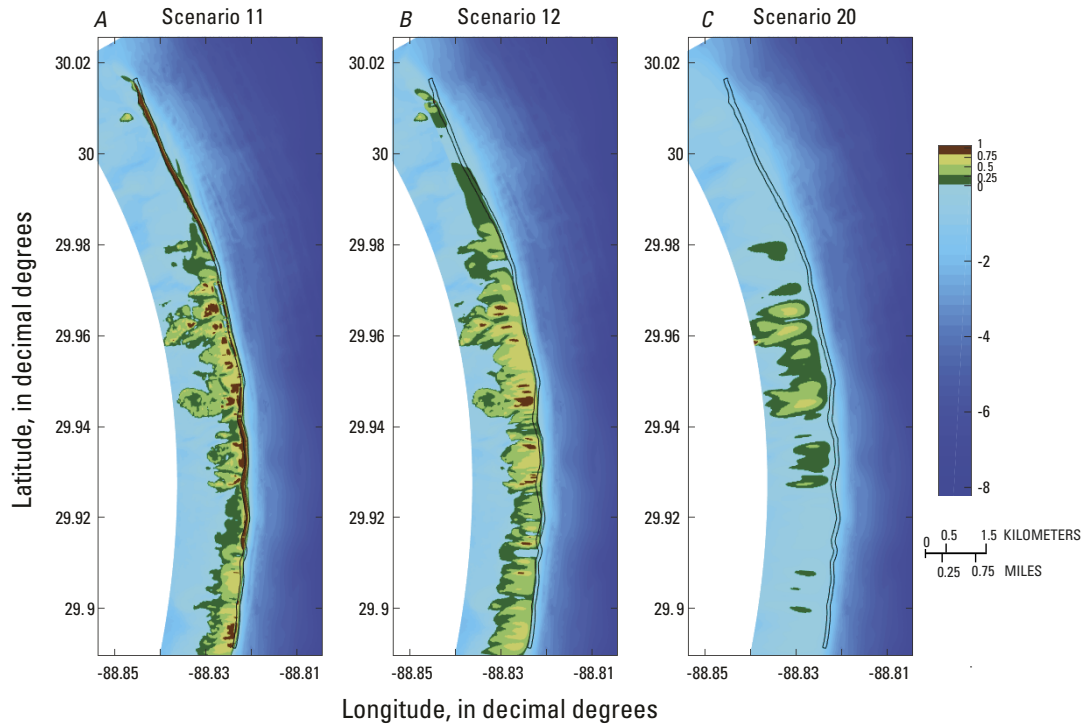
Results

Modeled post-storm DEMs were generated from the XBeach output to examine the morphologic change to the berm structure for each storm scenario and are provided in Mickey and others (2016). These DEMs can be used to identify erosional and depositional patterns, changes in barrier island shape and configuration, and areas that are considered vulnerable or resilient to storm impacts. Modeled DEMs illustrating the resultant bathymetry and topography from each of the nine scenarios simulated are shown in figures 7–9. Topographic changes are relatively subtle for scenarios 1–8, with the exception of a small heavily eroded area in the berm (fig. 7A red arrow) that appears in all scenarios. More extreme changes are apparent in scenarios 11–20, where breaching of the berm is prevalent and the island is largely washed away (scenario 20). The progressive impacts of the increasing storm scenarios can be seen in more detail when changes to a single profile are extracted from the DEMs (fig. 10).
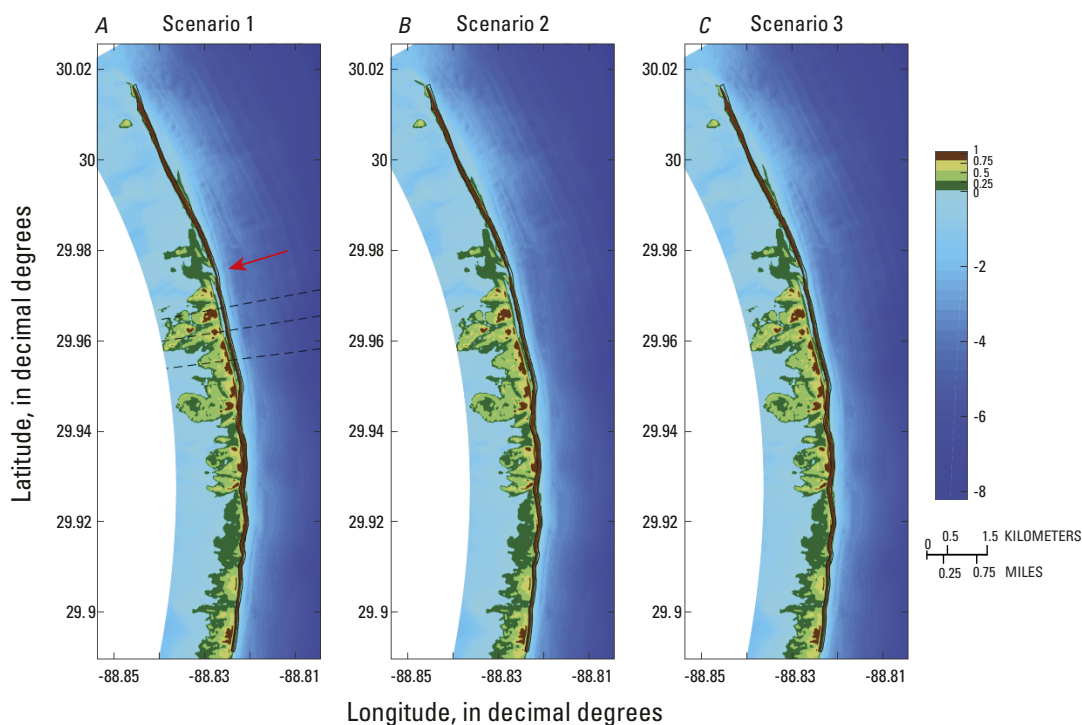
Figure 7. Digital elevation model (DEM) of the resulting bathymetry and topography, in meters, for (A) scenario 1, (B) scenario 2, and (C) scenario 3. Berm footprint outlined in black polygon. The red arrow in (A) identifies heavily eroded area of the berm for all scenarios. Black dashed lines show positions of profiles in figure 10.
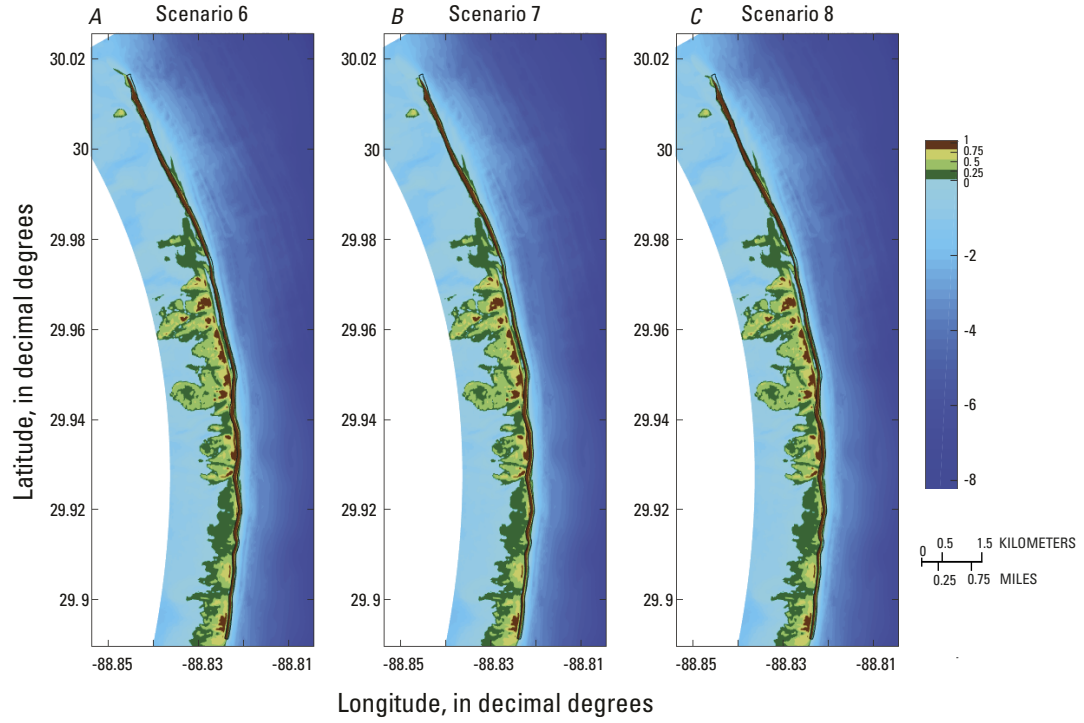
Figure 8. Digital elevation model (DEM) of the resulting bathymetry and topography, in meters, for (*A*) scenario 6, (*B*) scenario 7, and (*C*) scenario 8. Berm footprint outlined in black polygon.
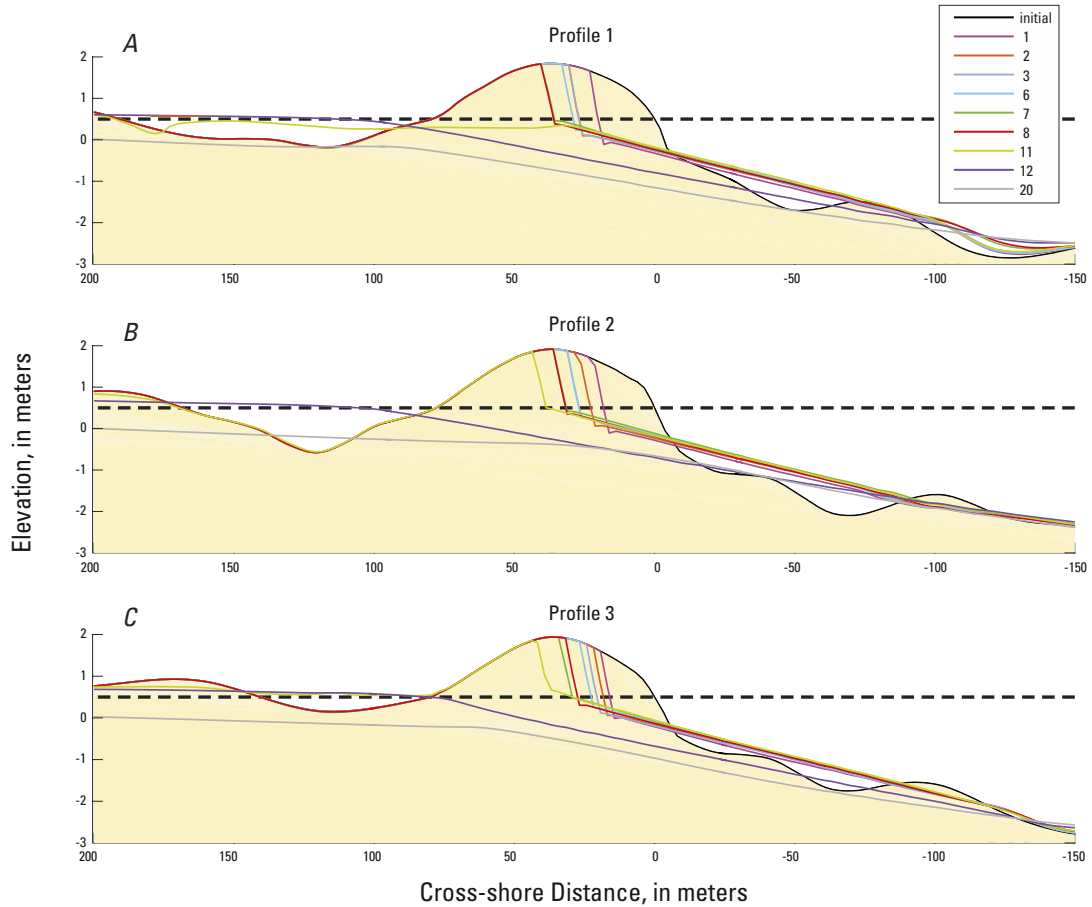

Figure 9. Digital elevation model (DEM) of the resulting bathymetry and topography, in meters, for (*A*) scenario 11, (*B*) scenario 12, and (*C*) scenario 20. Berm footprint outlined in black polygon.

Figure 10. Cross-shore transects of (*A*) profile 1, (*B*) profile 2, and (*C*) profile 3 [dashed lines north to south in figure 7*A*]. The colored lines indicate the final profile shape at the end of each of the nine scenarios, as well as the beginning shape indicated by the black line. The dashed line represents the 0.5 meter elevation threshold used for area and volumetric analysis.

Discussion

Model results provide an estimate of morphologic change and indicate how the idealized berm and surrounding island features respond to varying magnitudes of storm impacts that are characterized by historical observations for the northern Gulf of Mexico. Response ranged from berm collision and erosion in the low TWL scenarios (e.g., 1–8) to complete overwash and inundation in the high TWL scenarios (e.g., 11–20) (fig. 10). Significant impacts to the berm occurred in the scenarios where TWL reached above the 2 m threshold (e.g., 11–20), and the observable trend from these scenarios is that longer durations lead to more erosion. Quantitative analyses on the amount of change could be implemented by examining the differences in pre- and post-storm berm height, width, and area within the berm footprint at select profiles, for specific sections of the berm, or for the entire footprint. Thus, the effectiveness of existing or proposed restoration approaches can be quantified and compared to management objectives.

Although the storm scenarios are intended to be representative of actual storm conditions, these scenarios are not necessarily equivalent to specific storms. Nonetheless, it appears that some of the predictions match well with actual observed storm impacts to the Chandeleur Islands berm. The results from all scenarios reveal one distinct area of the berm feature (red arrow in fig. 7*A*) that was heavily eroded by wave collision in scenarios 1–8 and one of the first sites of overwash in scenarios 11–20,

11

indicating a location with relatively high vulnerability to a range of storm conditions. The same area was observed to overwash during construction of the berm (fig. 11). This suggests that (1) the modeling framework may be accurate enough to identify actual vulnerabilities, and (2) it may not be necessary to overly refine a set of scenarios in order to identify vulnerable areas.

Figure 11. Landsat imagery of the berm on January 12, 2011, with a water level of 0.05 meter (NAVD 88). Green dot on red line indicates the location of the northern tip of the original constructed berm, showing a breach between the northern and middle sections of the berm (red arrow).

Model identification of an observed vulnerable point suggests that the storm-impact approach could be implemented iteratively such that restoration project designs or other planned management responses can be modified on the basis of the outcome of the initial model simulations, and those modifications can be reassessed with new simulations. The storm-impact approach could also be applied cumulatively to a feature to determine the resiliency to multiple storm impacts versus the impacts of a single storm, either with or without feature recovery processes. The method of developing a set of representative storms could also be expanded further through combination with future climate scenarios to provide coastal scientists and managers with a method for investigating how, for example, the combination of extreme storms and future sea-level rise will affect the existing or restored coastal environment.

Summary

The storm-impact modeling framework outlined in this study describes a methodology for generating a set of storms that is representative of the type of events that occur in a region. This set of storms was developed using total water levels, including wave runup, to identify events when water levels were expected to impact dune and berm features. In addition to characterizing the oceanographic conditions present at the shoreline during historical storms, the framework is also capable of quantitatively assessing the sensitivity of morphological response to storms across the parameter space represented in the scenario set. Storm scenarios are simulated using a two-dimensional, process-based numerical model to estimate the alongshore variable morphologic change to the entire barrier island. Combining the development of a set of representative storms and morphological simulations at a specific region of interest allows assessment of storms that have affected the area in the past, providing information that can be used as part of coastal restoration projects to develop and modify restoration plans on the basis of the estimated morphologic change for similar storms that may occur in the future.

Acknowledgments

Information Statement

Although these data were processed successfully on a computer system at the U.S. Geological Survey, no warranty expressed or implied is made regarding the display or utility of the data on any other system, or for general or scientific purposes, nor shall the act of distribution imply any such warranty. The U.S. Geological Survey shall not be held liable for improper or incorrect use of the data described and (or) contained herein. Any use of trade, firm, or product names is for descriptive purposes only and does not imply endorsement by the U.S. Government.

References Cited

Bender, M.A., Knutson, T.R., Tuleya, R.E., Sirutis, J.J., Vecchi, G.A., Garner, S.T., and Held, I.M., 2010, Modeled impact of anthropogenic warming on the frequency of intense Atlantic hurricanes, Science, v. 327, p. 454–458, accessed August 15, 2016, at https://doi.org/10.1126/science.1180568.

DeWitt, N.T., Pfeiffer, W.R., Bernier, J.C., Buster, N.A., Miselis, J.L., Flocks, J.G., Reynolds, B.J., Wiese, D.S., and Kelso, K.W., 2014a, Coastal bathymetry data collected in 2011 from the Chandeleur Islands, Louisiana (version 2.0, July 21, 2015): U.S. Geological Survey Data Series 848, 1 DVD, accessed April 26, 2016, at https://doi.org/10.3133/ds848.

DeWitt, N.T., Pfeiffer, W.R., Miselis, J.L., Bernier, J.C., Reynolds, B.J., Wiese, D.S., and Kelso, K.W., 2014b, Coastal bathymetry and backscatter data collected in 2012 from the Chandeleur Islands, Louisiana: U.S. Geological Survey Data Series 847, accessed April 26, 2016, at https://doi.org/10.3133/ds847.

Fearnley, S., Miner, M., Kulp, M., Bohling, C., Martinez, L., and Penland, S., 2009, Hurricane impact and recovery shoreline change analysis and historical island configuration—1700s to 2005, chap. A *of* Lavoie, Dawn, ed., Sand resources, regional geology, and coastal processes of the Chandeleur Islands coastal system—An evaluation of the Breton National Wildlife Refuge: U.S. Geological Survey Scientific Investigations Report 2009–5252, p. 7–26.

Fredericks, X., and Plant, N.G., 2016, EAARL coastal topography—Chandeleur Islands, Louisiana, 4–5 September 2010—Seamless (bare earth and submerged): U.S. Geological Survey data release, accessed September 20, 2016, at https://doi.org/10.5066/F7W95785.

Guy, K.K., Doran, K.J., Stockdon, H.F., and Plant, N.G., 2014a, Topographic lidar survey of the Alabama, Mississippi, and Southeast Louisiana barrier islands, from September 5 to October 11, 2012: U.S. Geological Survey Data Series 839, 1 p., accessed April 26, 2016, at https://doi.org/10.3133/ds839.

Guy, K.K., and Plant, N.G., 2014, Topographic lidar survey of Dauphin Island, Alabama and Chandeleur, Stake, Grand Gosier and Breton Islands, Louisiana, July 12–14, 2013: U.S. Geological Survey Data Series 838, 1 p., accessed April 26, 2016, at https://doi.org/10.3133/ds838.

Guy, K.K., Plant, N.G., and Bonisteel-Cormier, J.M., 2014b, Topographic lidar survey of the Chandeleur Islands, Louisiana, February 6, 2012: U.S. Geological Survey Data Series 840, 1 p., accessed April 26, 2016, at https://doi.org/10.3133/ds840

Hasselmann, K., Barnett, T.P., Bouws, E., Carlson, H., Cartwright, D.E., Enke, K., Ewing, J.A., Gienapp, H., Hasselmann, D.E., Kruseman, P., Meerburg, A., Müller, P., Olbers, D.J., Richter, K., Sell, W., and Walden, H., 1973, Measurements of wind-wave growth and swell decay during the Joint North Sea Wave Project (JONSWAP): Hamburg, Germany, Deutsches Hydrographisches Institut Ergänzungsheft zur Deutschen Hydrogrphischen Zeitscrift Reihe A, v. 8, no. 12, 95 p.

Kindinger, J.L., Buster, N.A., Flocks, J.G., Bernier, J.C., and Kulp, M.A., 2013, Louisiana Barrier Island Comprehensive Monitoring (BICM) Program summary report—Data and analyses 2006 through 2010: U.S. Geological Survey Open-File Report 2013–1083, 86 p., accessed February 18, 2016, at http://pubs.usgs.gov/of/2013/1083/.

Long, J.W., de Bakker, A.T.M., and Plant, N.G., 2014, Scaling coastal dune elevation changes across storm-impact regimes: Geophysical Research Letters, v. 41, no. 8, p. 2899–2906, accessed August 1, 2016, at https://doi.org/10.1002/2014GL059616.

Louisiana Department of Natural Resources, 2010, U.S. Army Corps of Engineers joint permit application for work within the Louisiana coastal zone, accessed November 28, 2016, at http://dnr.louisiana.gov/assets/OCM/permits/JPA2010Fillable.pdf.

Mickey, R.C., Long, J.W., Thompson, D.M., Plant, N.G., and Dalyander, P.S., 2016, Storm-impact scenario XBeach model input and results: U.S. Geological Survey data release, accessed February 16, 2017, at https://doi.org/10.5066/F72F7KJK.

Penland, S., Suter, J., Sallenger, A., Jr., Williams, S., McBride, R., Westphal, K., Reimer, P., and Jaffe, B., 1989, Morphodynamic signature on the 1985 hurricane impacts on the northern Gulf of Mexico: Proceedings of the Symposium on Coastal and Ocean Management, v. 5, p. 4220–4234.

Plant, N.G., Edwards, K.L., Kaihatu, J.M., Veeramony, Jayaram, Hsu, Larry, and Holland, K.T., 2009, The effect of bathymetric filtering on nearshore process model results: Coastal Engineering, v. 56, p. 484–493.

Plant, N.G., Flocks, James, Stockdon, H.F., Long, J.W., Guy, Kristy, Thompson, D.M., Cormier, J.M., Smith, C.G., Miselis, J.L., and Dalyander, P.S., 2014, Predictions of barrier island berm evolution in a time-varying storm climatology: Journal of Geophysical Research—Earth Surface, v. 119, p. 300–316, accessed December 10, 2015, at https://doi.org/10.1002/2013JF002871.

Plant, N.G., and Guy, K.K., 2013a, Change in the length of the northern section of the Chandeleur Islands oil berm, September 5, 2010, through September 3, 2012: U.S. Geological Survey Open-File Report 2013–1074, 9 p., accessed May 10, 2016, at http://pubs.usgs.gov/of/2013/1074/.

Plant, N.G., and Guy, K.K., 2013b, Change in the length of the middle section of the Chandeleur Islands oil berm, November 17, 2010, through September 6, 2011: U.S. Geological Survey Open-File Report 2013–1075, 8 p., accessed May 10, 2016, at http://pubs.usgs.gov/of/2013/1075/.

Plant, N.G., and Guy, K.K., 2014, Change in the length of the southern section of the Chandeleur Islands oil berm, January 13, 2011, through September 3, 2012: U.S. Geological Survey Open-File Report 2013–1303, 8 p., access May 10, 2016, at http://pubs.usgs.gov/of/2013/1303/.

Roelvink, Dano, Reniers, Ad, van Dongeren, Ap, van Thiel de Vries, Jaap, McCall, Robert, and Lescinski, Jamie, 2009, Modelling storm impacts on beaches, dunes and barrier islands: Coastal Engineering, v. 56, p. 1133–1152.

Sallenger, A.H., Jr., 2000, Storm impact scale for barrier islands: Journal of Coastal Research, v. 16, no. 3, p. 890–895, accessed September 15, 2016, at http://coastal.er.usgs.gov/hurricanes/publications/jcr.pdf.

Stockdon, H.F., Holman, R.A., Howd, P.A., and Sallenger, A.H., Jr., 2006, Empirical parameterization of setup, swash, and runup: Coastal Engineering, v. 53, no. 7, p. 573–588.

U.S. Fish & Wildlife Service, 2013, Breton National Wildlife Refuge Web page: U.S. Fish & Wildlife Service, accessed April 26, 2016, at https://www.fws.gov/breton/.

Wahl, T., and Plant, N.G., 2015, Changes in erosion and flooding risk due to long-term and cyclic oceanographic trends: Geophysical Research Letters, v. 42, no. 8, p. 2943–2950.

Williams, S.J., 2009, Past, present, and future sea level rise and effects on coasts under changing global climate, chap. C *of* Lavoie, Dawn, ed., Sand resources, regional geology, and coastal processes of the Chandeleur Islands coastal system—An evaluation of the Breton National Wildlife Refuge: U.S. Geological Survey Scientific Investigations Report 2009–5252, p. 37–46.

Appendix 1. Example Model Input Files

Example XBeach input file for the scenario simulations is provided in this appendix. The example file shown is for Scenario 1; all other scenario input files follow this same setup with only a few lines changed for the inputs of "tstop," "bcfile," "zs0file," and "zsinitfile."

Params.txt:

```
Bin 1 : Duration(8hrs) TWL(>1.013)
Physical processes
sedtrans   = 1
morphology = 1
single_dir = 1

Grid parameters
nx       = 639
ny       = 1149
vardx    = 1
xfile    = x_imageBerm.grd
yfile    = y_imageBerm.grd
depfile  = z_imageBerm.dep
posdwn   = -1
thetanaut = 1
thetamin = 0
thetamax = 180

Single direction
dtheta_s = 10
wavint = 600

Model time
tstop = 208800

Wave boundary condition parameters
instat = jons_table
bcfile  = jonswap1.txt

Flow boundary condition parameters
front   = abs_2d
back    = abs_2d
left    = neumann
right   = neumann

Tide boundary conditions
tideloc = 2
paulrevere = 0
zs0file = Bin_1_waterlevel.dat
zsinitfile = zsinit_1.dat
```

```
Bed composition parameters
rhos = 2650.0
D50  = 0.000163
D90  = 0.000253

Morphology parameters
morfac   = 10
smax     = 1

outputformat  = netcdf

Output variables
timings = 1
tstart  = 3600
tintg   = 3600
tintm   = 3600
tintp   = 5

nrugauge  = 0
rugdepth  = 0
ncross    = 0
nglobalvar = 10
H
u
v
zb
hh
zs
Susg
Svsg
Subg
Svbg

nmeanvar = 9
H
u
v
Susg
Svsg
Subg
Svbg
zs
DR
```

≋USGS

Mickey and others—**A Methodology for Modeling Barrier Island Storm-Impact Scenarios**—Open-File Report 2017–1009, ver. 1.1